An Aircraft Hybrid Electric Propulsion Model Experimentally Validated

1st Enrico Fornaro
Department of Industrial Engineering
University of Naples "Federico II"
Naples (80125), Italy
enrico.fornaro@unina.it

2nd Massimo Cardone
Department of Chemical, Material, and Production Engineering
University of Naples "Federico II"
Naples (80125), Italy
massimo.cardone@unina.it

3rd Valerio D'Agostino
Department of Industrial Engineering
University of Naples "Federico II"
Naples (80125), Italy
valerio.dagostino2@unina.it

4th Adolfo Dannier
Department of Electrical Engineering, and Information Technologies
University of Naples "Federico II"
Naples (80125), Italy
adolfo.dannier@unina.it

***Abstract*— In this paper a Matlab/Simulink model of a Hybrid Electric Propulsion System (HEPS) for aircraft application is presented. An Electric Machine (EM) is mechanically coupled to Internal Combustion Engine (ICE) via a one-way bearing to obtain a parallel hybrid propulsion configuration. Numerical modelling and experimental validation of the system have been carried out; the experimental data were acquired on propulsion prototype installed on test bench at University of Naples Federico II. Before implementing the entire powertrain model in Matlab/Simulink environment, the experimental characterizations of single systems, ICE and EM, in terms of performance and efficiency have been done. Furthermore, the proposed model also contains a generic dynamic sub model of rechargeable lithium-ion batteries that represents the most popular types of accumulators currently used in propulsion systems. The entire model was validated by the experimental data obtained during a quick mission of aircraft simulated on test bench. To confirm the good matching between experimental and simulated data of proposed model, two different statistical indexes are also evaluated. The results of the experimental and simulated activities show the completely feasibility of the designed hybrid electric propulsion system architecture. Finally, the model provides a smart, easy, fast tool to implement any control strategies to enhance fuel consumption, CO_2 and pollutant emissions, which are the main goals of the hybrid solutions of transportation sector.**

Keywords — SI engine, electric machines, Simulink model, aviation, hybrid propulsion, mission simulation

I. INTRODUCTION

The contribution of civil aircraft transport systems to CO_2 emissions and its associated greenhouse gas (GHG) emissions stood at 2% in 2020 [1] and without proactive measures, these emissions are projected to increase by 3-4% annually, in line with the growth of the aviation industry. Therefore, environmental issues in this field such as noise, emissions, and fuel consumption are becoming important for energy and environmental sustainability [2].

The International Civil Aviation Organization, aligning with COP21 guidelines, implement a series of measures to reduce the environmental impact of aircraft on climate change, particularly in reducing CO_2 emissions [3].

The EU Commission's strategic vision, as outlined in Flightpath 2050 [4], advocates for full-electric (FEPS) and hybrid-electric (HEPS) propulsion systems as potential solutions to reduce CO_2 emissions and address climate impacts. HEPS and FEPS technologies are expected to compete favourably with other propulsion systems such as biofuels and hydrogen [5]. However, these alternative fuel-based engine technologies are not yet fully developed and certified, leading the aviation industry to prioritize electrification of propulsion systems to create hybrid solutions [6].

HEPS architecture is generally preferred over FEPS due to challenges in storing electric energy in systems lighter than conventional fuel tanks [7]. Additionally, the flexibility to configure HEPS in different architectures enhances their versatility across various aircraft types [8]. Combining a conventional internal combustion engine (ICE) with electrical machines (EM) in HEPS offers advantages such as noise reduction compared to ICE and improved endurance performance over FEPS [9].

The comparison between serial-hybrid and parallel-hybrid architectures in designing HEPS highlights the benefits of the parallel-hybrid solution, including reduced weight and electric energy conversion losses [10,11]. However, the parallel configuration introduce more complexity, necessitating a comprehensive strategy to manage ICE, EMs, and the energy storage system (ES) within the HEPS framework.

This work proposes a HEPS model designed in Matlab/Simulink experimentally validated. For this purpose, an experimental test has been conducted on real hybrid-electric prototype, where a short flight mission of the propulsion has been conducted in a test bed. Successively, the experimental data has been used to validate the hybrid powertrain consisting of an internal combustion engine, an electric machine, and the battery pack model linked to the dynamic model.

II. HYBRID SYSTEM ARCHITECTURE

The proposed architecture for the hybrid electric powertrain is set up in parallel, with the internal combustion engine (ICE) and electrical machine (EM), supplying power to the propeller in both directions (Figure 1). In this configuration, the propeller power P_{PROP} is calculated as follows.

$$P_{PROP} = P_{ICE} + P_{EM} \quad (1)$$

While P_{ICE} will be always positive, P_{EM} could be positive or negative depending on the flight phase of the aircraft. Typically, in take-off or climb phases, the EM works as a motor, while the EM works as a generator in descending or landing phases. Indeed, during the descending and landing phases, the ICE over-power could be employed to generate electrical energy to recharge the battery pack.

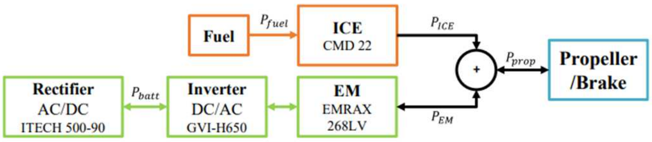

Figure 1. Scheme of the hybrid electric propulsion system

The following is a summary of four operational modes of the hybrid-electric propulsion system:

- *fuel-only*, in this case, ICE and EM are running, but only ICE transfer power to the propeller, while the EM running as a flywheel;
- *battery-only*, regarding this case, only the EM is running as a motor, and the propeller power is equal to the EM power;
- *hybrid*, in this case, both ICE and EM are running, and the propeller power is a sum of ICE and EM power;
- *charging*, concerning this case, ICE and EM are running, but the last one works as a generator to charge the battery, while the ICE provides power both to the propeller shaft and EM.

For this purpose, a high power density permanent magnet synchronous machine (PMSM) has been chosen that guarantees at 2750 rpm a continuous power of 62 kW and good efficiency around 95-96%. Moreover, applying the following equation is possible to calculate the degree of hybridization (DoH) of the current HEPS prototype:

$$DoH_p = \frac{P_{EM}}{P_{ICE}+P_{EM}} = \frac{62}{62+95} \sim 0.4 \qquad (2)$$

The ICE used in this work is a twin Spark Ignition naturally aspirated and air-cooled unit manufactured by the CMD Engine S.p.a. (a Loncin Company), developed for light and general aviation aircraft, named CMD 22. All specifications are summarized in Figure 2 [12].

Technical specification	UoM	CMD 22
Bore	mm	100
Stroke	mm	70
Displacement	cm^3	2198
Compression ratio	-	9,7:1
Cylinder N°	-	4
Prop. drive ratio	-	1:2
Dry Weight m_{ICE}	kg	77,6
Weight/Power	kg/Hp	0,657
Max.Power (@5500rpm)	kW	95
Max.Torque(@5500rpm)	Nm	175

Figure 2. Internal combustion engine CMD 22: technical specifications [12]

The EM used in this work is the EMRAX 268 Low Voltage, manufactured by the Electric Motor Roman AXial EMRAX d.o.o. It has been developed and produced for the aerospace industry (all specifications are highlighted in Figure 3 [13]). The best characteristics of EMRAX motors are respectively lightweight best-in-class power density (up to 10 kW/kg), high efficiency (up to 98%), high torque at low speed, and reliability.

Technical specification	UoM	EMRAX 268 LV
Weight	kg	20
Diameter/Width	mm	268/91
Max. battery voltage	Vdc	250
Continuous Power	kW	107 CC
Peak Power	kW	200
Continuous Torque	Nm	250 CC
Peak Tower	Nm	500
Max. Speed	rpm	4500
Continuous Current	Arms	500
Peak Current	Arms	1000
Motor efficiency	%	92-98
N° pole pairs	-	10
Rotor Inertia	Kgm^2	0.0922
Wire connection	-	star
Induction Lq/Ld	µH	17/15.9
Magnetic flux - axial	Vs	0.0245
Specific load speed	rpm/1Vdc	18

Figure 3. PMSM EMRAX 268 LV: technical specifications [13]

The power supply consists of a bi-directional programmable AC/DC (Rectifier) IT6018C-500-90, which adopts the SiC-base technology, manufactured by the ITECH (all specifications are highlighted in Figure 4). This module offers the functionality of two-quadrant operation shown in Figure 5. The regenerative capability ensures to put back of the energy onto the grid [15]. As reported in the technical specifications in Figure 4, the maximum power that it's possible to transfer to EM is limited to 18 kW.

Technical specification	UoM	IT6018C-500-90
AC Input Voltage	Vac	198 to 264
AC Input Frequency	Hz	47 to 63
DC Output Voltage	Vdc	0 to 500
DC Output Current	A	-90 to 90
DC Output Power	kW	-18 to 18
Efficiency	%	92
Operating Temperature	°C	0 - 50
Weight	kg	40
Communication	-	USB, CAN, LAN
Internal resistance	Ω	~1

Figure 4. Bidirectional programmable AC/DC power supply IT6018C-500-90: technical specifications [14]

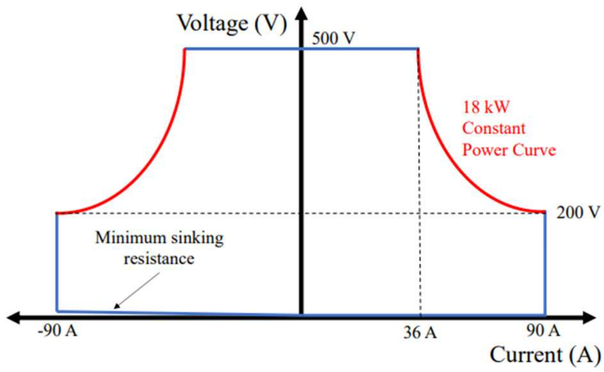

Figure 5. Auto ranging output of a 18 kW bi-directional power supply. Maximum voltage [15]

Moreover, an essential component of a parallel hybrid-electric propulsion system is the mechanical clutch. This component is able to combine the power of the ICE and EM. The one-way bearings are a cheaper, simpler, reliable, and lighter solution regarding the electromagnetic clutch or planetary gearing. Furthermore, the one-way bearing is a good compromise choice for this prototype concept HEPS, guaranteeing compliance with the requirements.

In order to obtain an experimental characterization of efficiency map of EM and BSFC map of ICE and for further validation, an eddy-current brake is employed. It allows to simulate several missions, running in three possible "brake control modes" respectively:

- $N = k$ the brake speed is fixed (used during experimental efficiency characterization).
- $M = k$ the brake torque is fixed.
- Mn^2 is typical square load seams to the marine and aeronautical propellers where the braking torque is proportional to the current.

All mechanical power is converted into heat one (joule effect) subtracted through a closed-loop cooling circuit employing water as a heat carrier.

III. Experimental Characterization

The hybrid electric propulsion prototype for aircraft application has been realized in the laboratory of Department of Industrial Engineering of the University of Naples Federico II [16]. The performances characterization of EM and ICE has been made with several tests on test bed. This step is essential for the input set information to design Matlab/Simulink model.

Firstly, an investigation of the electrical efficiency of the coupling EM and inverter has been carried out. In particular, a comparison between the measured efficiencies and the values provided in the EMRAX 268 datasheet has been made. The electrical efficiency has been calculated in an indirect way, starting from electrical DC measures of Current (A) and Voltage (V), and mechanical measures of torque and speed. In particular, the speed range has been selected of 250 to 2750 rpm in increments of 250 rpm. Moreover, the torque value has been changed between 10 and 150 Nm. Due to the limited power of the bi-directional converter ITECH (only 18 kW), some tests at high speed and torque haven't been performed. All the tests have been realized adopting a fixed speed controller ($N = k$), maintaining the brake speed at a constant rotational value. Comparing the experimental results of the electrical efficiency (highlighted in dashed red box) with the datasheet values of the EMRAX 268 motor, as shown in

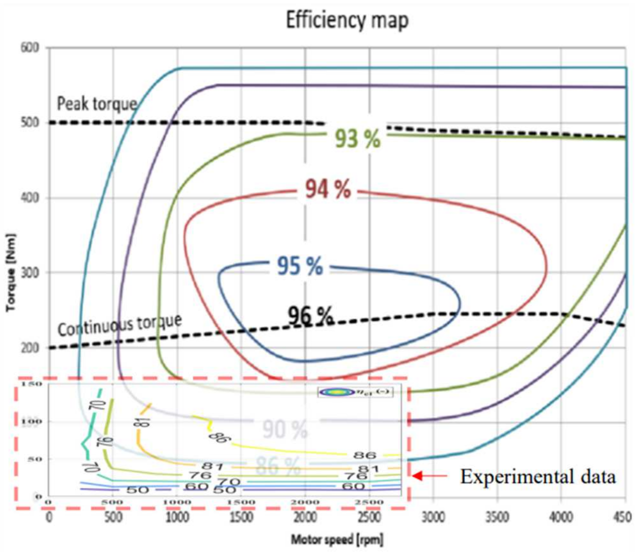

Figure 6. EMRAX 268 efficiency map [13]. In dashed red transparency box

Figure 6, can be observed: concerning the 86% isoline a matching between the two sets of data (experimental and datasheet) for higher rotational speeds around 2500 to 2000 rpm; for lower rotational speeds ranging from 500 to 1500 rpm, the difference consistently increases as the rotational speed decreases.

This difference could be ascribed to various factors:

a) *Magnetic Polarization* – In a Permanent Magnet Synchronous Motor (PMSM), efficiency is conditioned by the polarization of permanent magnets and their alignment with the motor's windings. At lower speeds, the magnetic field might not be fully aligned with the windings, leading to losses in magnetic flux and reducing the efficiency.
b) *Motor Control* – The control of a PMSM is often optimized for a definite speed range. Generally, the inverter has different control strategies that can changed at low speeds, which may not be as efficient as those used at higher speeds.
c) *Overall Efficiency* – The experimental efficiency data pertains to the combination of the inverter and the electric machine. The datasheet value only refers to the electric machine itself.
d) *Cooling system* – In the conducted tests, the electric machine was cooled using only air, without the water cooled. The EMRAX declared to use both cooling systems.

These factors can contribute to the observed differences in efficiency between the experimental results and the datasheet values for the EMRAX 268 motor.

The internal combustion engine is mechanically coupled to the electric machine via a one-way bearing. In the "*fuel-only*" mode, the power is generated by the internal combustion engine, and, at the same time, the electric machine remains connected to the driveline placed in rotation, behaving as a flywheel. In order to compute BSFC map of ICE, several tests have been made at steady-state points and the brake control has been fixed in $N = k$ mode with a discrete torque switch. For each point the BSFC has been calculated (Equation 3) as fuel consumption rate and mechanical power ratio, as follows:

$$BSFC\left(\frac{g}{kWh}\right) = \frac{Fuel\ Consumption\ Rate\left(\frac{l}{h}\right) * 1000 * \rho_{gasoline}}{P_{ICE}} \qquad (3)$$

where $\rho_{gasoline}$ represents the gasoline density (750 g/l).

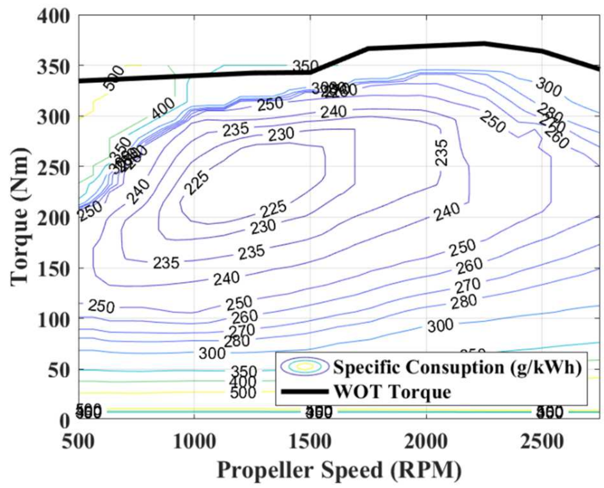

Figure 7. CMD 22 Brake specific fuel consumption (BSFC) (g/kWh)

IV. POWERTRAIN MODEL

Numerical modelling and experimental validation have been applied to the aircraft HEPS, which has been realized and experimentally assessed at the test bed, as previously described. The numerical validation of the entire model has been carried out based on the experimental data obtained during the test execution of the flight mission [17].

For this purpose, the HEPS model, shown in Figure 8, has been designed in the Matlab/Simulink environment, consisting of the main blocks:

- *Hybrid Propulsion* - Mainly constituting of ICE, EM and Battery, it is green block in the model scheme shown in the figure. The models of each components has been provided;
- *Brake Curve*;
- *Dynamic Model*.

Hybrid Propulsion

The model inputs are the torque required by the ICE (EngTrq_exp) and the torque required by the EM (MtrTrq_exp) respectively [18].

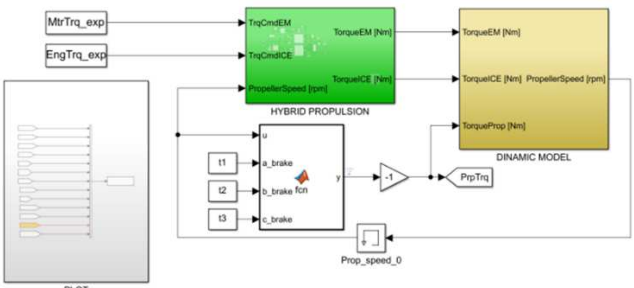

Figure 8. Hybrid Propulsion Model in Matlab/Simulink

Figure 9 shows the inside of the Hybrid Propulsion block, which represents the heart of the propulsion system, where the internal combustion engine and the electric motor have been modelled as a Map, employing the experimentally acquired performance data collected on a dedicated test rig. The Matlab Mapped SI Engine block is used to implement the experimental CMD22 torque and the brake specific fuel consumption (BSFC) [19]. A similar approach has been adopted for the EM where the Matlab Mapped Motor/Generator block has been used to implement the EMRAX 268 torque and efficiency [20].

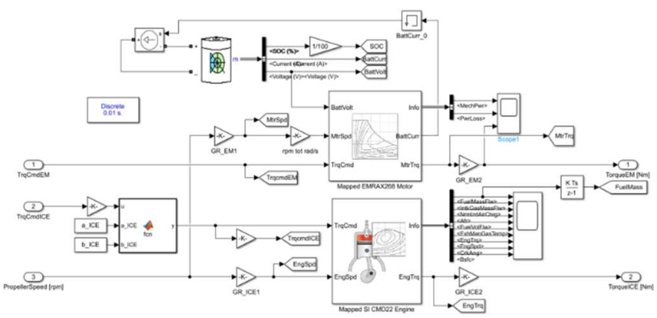

Figure 9. Hybrid Propulsion Block

Moreover, the battery voltage V_{batt} is modelled using the Simulink battery block [21]. This block provides a generic dynamic model that simulates the most popular types of rechargeable batteries. In this study, a Lithium-Ion pack battery has been modelled. To avoid complexity, the battery aging effect isn't taking into account. The discharge and charge model has been described through equations 4 and 5 [22-23], where i represents the charging/discharging current, $i*$ is the filtered current value, Q is the all battery pack capacity, and it is the current time integral plus the initial battery charge. In Figure 10 the most important parameters E_0, R, K, A and, B considered in this model have been shown, and in the same figure the discharge model of the battery pack is represented.

- Discharge ($i^* > 0$)

$$V_{batt} = E_0 - R \cdot i - K \frac{Q}{Q-it}(i^* + it) + A \cdot \exp(-B \cdot it) \quad (4)$$

- Charge ($i^* < 0$)

$$V_{batt} = E_0 - R \cdot i - K \frac{Q}{Q-0.1 \cdot it} i^* + -K \frac{Q}{Q-it}(i^* + it) + A \cdot \exp(-B \cdot it) \quad (5)$$

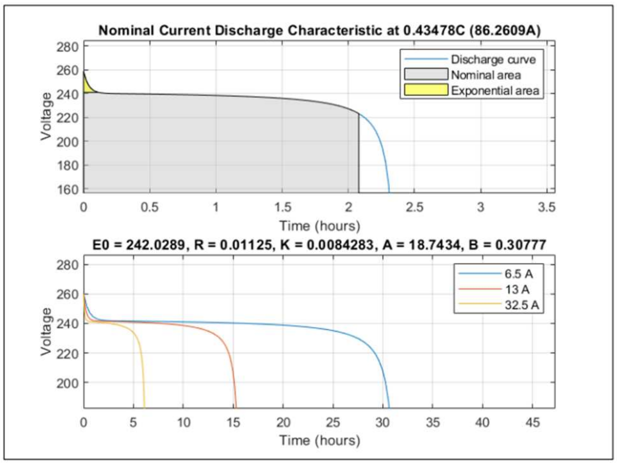

Figure 10. Battery pack discharge characteristic model

Brake Curve

The Brake Curve, due to the propeller load, has been experimentally simulated by setting the control of the brake to the Mn²=k mode. The numerical equation referred to the brake load has been evaluate through a best fitting starting form experimental data (speed, torque, power). Hence, the numerical torque $T(n)$ and power $P(n)$ curves are following described:

$$T(n) = t1 \cdot n^2 + t2 \cdot n + t3 \quad (6)$$

where $t1 = 8.94 - 0.6$; $t2 = 0.075$; $t3 = 82.65$

$$P(n) = p1 \cdot n^3 + p2 \cdot n^2 + p3 \cdot n + p4 \quad (7)$$

where $p1 = 9.59 - 10$; $p2 = 7.8 - 6$; $p3 = 0.0087$; $p4 = -0.013$
and n is rotational speed of propeller in rpm.

The representations of the previous two curve have been shown Figure 11 reported below.

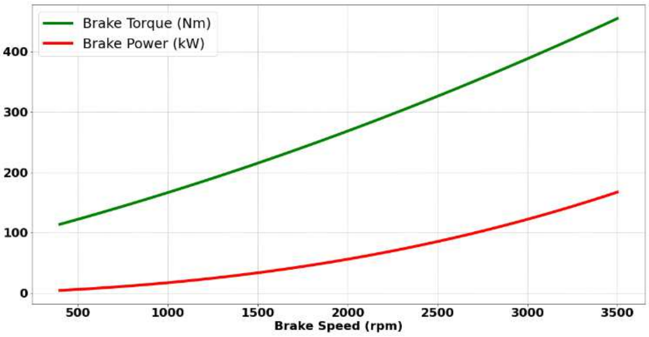

Figure 11. Simulated Brake Torque and Brake Power

Dynamic Model

Finally, the Dynamical Model has been modelled using the torque balance Equation 8 and discretizing this equation is possible estimate the propeller speed velocity through the Equation 9.

$$T_{ICE} + T_{EM} - T_{PROP} = I\frac{d\omega}{dt} \cong I\frac{\omega_f - \omega_i}{t_f - t_i} \quad (8)$$

$$\omega_f = (T_{ICE} + T_{EM} - T_{PROP}) \cdot \frac{\Delta t}{I} + \omega_i \quad (9)$$

Where, T_{ICE} is the ICE torque, T_{EM} is the EM torque (positive when EM work as a motor, negative work as a generator), T_{PROP} is the propeller's resistant torque, I is the system's overall moment of inertia, and ω is the propeller angular speed in rad/s. The moment of inertia (Table 1) is sum of three components: I_{EM} has been given by the manufacturer's EM datasheet; in this case, I_{PROP} has been replaced by the brake dynamometer moment of inertia; the remaining moment of inertia (ICE, pulleys, and free wheel inertia) has been obtained through a parameter estimator process and reflected to the propeller shaft.

Table 1. Summary of Moment of Inertia

Description	UoM	Inertia
EMRAX 268	kgm^2	0.0922
EDDY BRAKE SCHENK	kgm^2	0.61
CMD22 and mech. coupling	kgm^2	0.3

V. Mission Simulation

In order to validate the matching between model and experimental data a mission has been chosen. It is a short flight mission, repeated twice, where HEPS is utilized in hybrid and charging operating modes. The control of the brake has been set at $Mn^2 = k$ mode. The mission is divided into two main parts, and each part consists of the following phases, summarized in Table 2:

1. *Taxi* – the HEPS operates in hybrid mode, the operating point is set at 32 kW at 1400 rpm. The taxi phase wasn't repeated in the second part of the mission.
2. *Take-off* – the HEPS operates in hybrid mode, the operating point is set at Take-off performances 87 kW at 2500 rpm.
3. *Climb* – the HEPS operates in hybrid mode, the operating point is set at Max. Continuous Power 78 kW at 2380 rpm.
4. *Cruise* – the HEPS operates in hybrid mode, and the operating point is set at 75% Max. Continuous Power 58 kW at 2050 rpm.
5. *Approach and Landing* – the HEPS operates in charging mode, at operating points with decreasing power. The second part of the mission is repeated like the first one (excluding the initial taxi part), assuming that at the end of the first landing, the pilot performs a manoeuvre known as a "*touch-and-go*". Additionally, it's assumed that the landing in the second phase is longer than the first, highlighting the operation of the HEPS in the charging mode.

Table 2. Table of Mission phases and duration

Mission Phase	Start Time (s)	Stop Time (s)	Duration (s)
Taxi	$t_0 = 0$	$t_1 = 24$	24
Take-off	$t_1 = 24$	$t_2 = 70$	46
Climb	$t_2 = 70$	$t_3 = 110$	40
Cruise	$t_3 = 110$	$t_4 = 265$	155
Approach & Landing	$t_4 = 265$	$t_5 = 390$	125
Take-off	$t_5 = 390$	$t_6 = 425$	35
Climb	$t_6 = 425$	$t_7 = 475$	50
Cruise	$t_7 = 475$	$t_8 = 615$	140
Approach & Landing	$t_8 = 615$	$t_9 = 728$	113

To bring the tested mission closer to reality, the IT9000 simulation software within the bi-directional power supply ITECH IT6018C-500-90 has been used to simulate the dynamic behavior of a Lithium-Ion battery. For this purpose, a battery pack has been designed with following cell specifications. The cells specification are based on the PANASONIC NCR18650B [24], as indicated in Figure 12. Finally, a battery pack is composed of 62s62p cells, with a nominal voltage of $Vnom = 225\ V$, a nominal capacity of $Cnom = 210\ Ah$, and a stored energy of $Enom = 47\ kWh$.

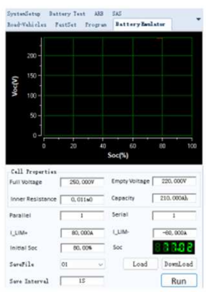

Technical specification	UoM	Data
CELL		
Full Voltage	V	4.2
Nominal Voltage	V	3.6
Empty Voltage	V	2.5
Inner Resistance	Ω	0.011m
Rated Capacity	Ah	3400m
PACK		
Parallel	-	62
Serial	-	62
Initial SoC	%	80
I_{max} (ITECH limit)	A	80
I_{min} (ITECH limit)	A	-80
V_{nom}	V	225
C_{nom}	Ah	210
E_{nom}	kWh	47

Figure 12. Cell Technical specification setting in IT9000 SW

VI. Results

In this section the results obtained from simulations made in the Matlab/Simulink environment of the hybrid-electric propulsion system designed for aircraft applications are illustrated. The data from the experimental test and the simulated one are compared in the clustered figures below (Figure 13).

The simulation solver is ode4 (Runge-Kutta), with a fixed step size $\Delta t = 0.01s$. Moreover, the initial value of propeller speed has been set equal to zero $\omega_0 = 0$, and the initial battery State of Charge (SoC) is set equal to 80%.

The speed trends in Figure 13 (a) are almost similar in EM, ICE and the brake, confirming the correct mechanical coupling constraints between all components. The EM torque comparison, in Figure 13 (b), confirm a good matching between the experimental and simulation one results. Otherwise, the ICE and brake torque shows more variation, which could be ascribed to a less ICE map accuracy, and a braking curve approximation. The battery trends shown in Figure 13 (c) are good.

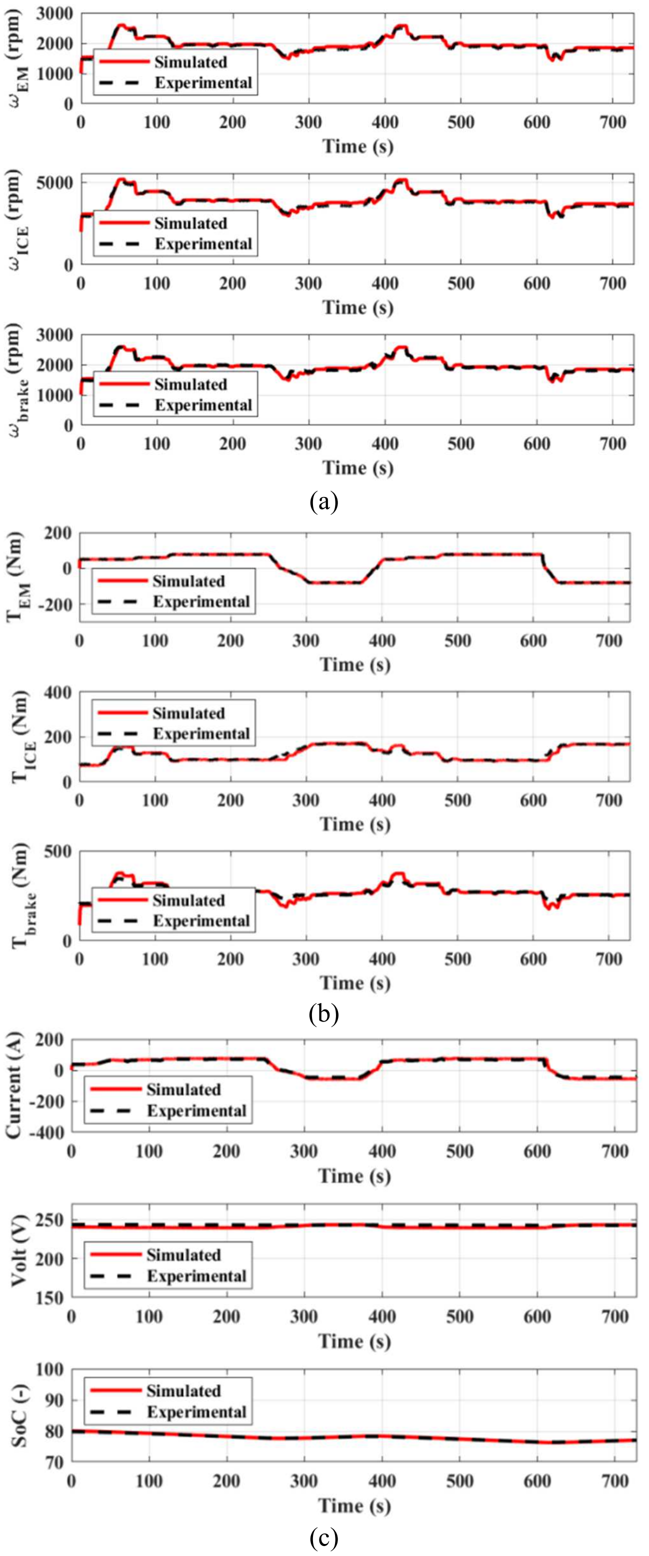

Figure 13. Comparison between experimental and simulated signals: (a) speed, (b) torque and (c) battery quantities

The simulated battery current and voltage variation with respect to experimental one can be attributed to a simple battery model chosen. In fact, the battery model does not take into account the thermal and aging behavior of the battery.

In all cases a good matching between the experimental and simulated curves has been highlighted. Moreover, same considerations are true for battery SOC, Current and Voltage. Two different statistical indexes are also calculated for a better performance analysis. These indexes are respectively, Root Mean Square Error (RMSE) and Normalized Root Mean Square Error (NRMSE). Normalizing the RMSE facilitates the comparison between datasets or models with different scales. Moreover, the NRMSE value is commonly expressed as a percentage where the normalization is referred to the magnitude variation range ($t_{max,k} - t_{min,k}$).

$$RMSE,_{k} = \sqrt{\frac{1}{N}\sum_{i=1}^{N}\left(t_{i,k} - y_{i,k}\right)^2} \tag{10}$$

$$NRMSE,_{k} = \frac{RMSE,_{k}}{t_{max,k} - t_{min,k}} \tag{11}$$

In Equations 10 and 11, $t_{i,k}$ are the reference values provided by the experimental tests, $y_{i,k}$ are the simulated value provided by the model. Moreover, the subscript k is referred to the different considered signal, summarized in Table 3.

Table 3. Goodness indexes of the modeling matching for Speed, Torque and Battery parameters

Signals	UoM	RMSE (UoM)	NRMSE (%)
Speed ICE	(rpm)	107.4	0.04
Speed EM	(rpm)	54.1	0.04
Speed Brake	(rpm)	48.41	0.04
Torque ICE	(Nm)	90.7	2.97
Torque EM	(Nm)	0.56	0.003
Torque Brake	(Nm)	14.0	0.49
Battery Current	(A)	7.7	0.06
Battery Voltage	(V)	2.6	2.54
Battery SoC	(-)	0.16	0.04

The values of NRMSE confirm the good matching of the proposed model with experimental data, the maximum percentage error is 2.97%, regarding to estimation of ICE torque that could be ascribed to a less ICE map accuracy, and 2.54%, regarding to estimation of battery voltage that could be ascribed to a simple battery model chosen.

VII. Conclusions

Simulation performances of hybrid-electric propulsion system model have been proposed in this work. In addition, a comparison between experimental data has been described in order to demonstrate, through the use of two statistical indexes, a good matching.

This activity has been conducted by simulating a short flight mission, with a little more than 12 minutes duration. Unfortunately, the maximum power exerted by EM was limited to 18 kW due to limitation imposed by characteristics of IT6018C-500-90 bi-directional programmable AC/DC power supply. The proposed mission has been conduced for efficiency characterization and validation phases.

Firstly, in order to obtain the necessary input data for designing a Matlab/Simulink model, an efficiency characterization of both the internal combustion engine and the electric motor was conducted. The model method used is map-based and it is appropriate for testing various motor setups. Furthermore, a model of Lithium-Ion batteries has been created to describe the energy storage mechanism. Finally, when compared to the experimental data, the simulation results from Matlab/Simulink model have shown that the suggested basic model was able to accurately forecast the behavior of the energy storage system and the parallel hybrid-electric propulsion system. This test highlights a proper designed model. It could be suitable for any further test to perform an energy management strategy to manage the power distributions among different motors power sources, optimizing the fuel consumption during the flight. The final goal of Matlab/Simulink model implementation is avoiding experimental tests to validate, for instance, any fuel economy strategies, obtaining similar results and involving much fewer resources.

Acknowledgment

This research has been realized during the DIPROVEL project for the development of Technology Demonstrator of an Aeronautical Hybrid Propulsion System for Light Aircraft Applications funded by the Italian Ministry of Economic Development (MISE).

The authors thank Mr. Salvatore De Cristofaro for his technical assistance in laboratory activities.

References

[1] Hu, S., Fruin, S., Kozawa, K., Mara, S., Winer, A. M., & Paulson, S. E. (2009). Aircraft emission impacts in a neighborhood adjacent to a general aviation airport in Southern California. Environmental science & technology, 43(21), 8039-8045.

[2] Burleson, C., & Maurice, L. (2003, July). Aviation and the environment: challenges and opportunities. In AIAA International Air and Space Symposium and Exposition: The Next 100 Years (p. 2554).

[3] Consolidated Statement of Continuing ICAO Policies and Practices Related to Environmental Protection A39-1 – General Provisions, Noise and Local Air Quality; A39-2 – Climate Change; A39-3 – Global Market-Based Measure (MBM) Scheme," ICAO, Montreal, 2016.

[4] European Commission, "Directorate General for Research and Innovation, & Directorate General for Mobility and Transport," Flightpath 2050: Europe's Vision for Aviation: Maintaining Global Leadership and Serving Society's Needs, 2011.

[5] Dincer, I. and Acar, C., "A Review on Potential Use of Hydrogen in Aviation Applications," International Journal of Sustainable Aviation 2, no. 1 (2016): 74-100.

[6] Gössling, S. and Humpe, A., "The Global Scale, Distribution and Growth of Aviation: Implications for Climate Change," Global Environmental Change 65 (2020): 102194.

[7] Isikveren, A.T., Fefermann, Y., and Maury, C., "Long-Term Hybrid-Electric Propulsion Architecture Options for Transport Aircraft," in Conference: Greener Aviation, Brussels, 2016.

[8] Finger, D.F., Götten, F., Braun, C., and Bil, C., "On Aircraft Design under the Consideration of Hybrid-Electric Propulsion Systems," in The Proceedings of the 2018 Asia-Pacific International Symposium on Aerospace Technology (APISAT 2018) 9th, 2019, 1261-1272.

[9] DelRosario, R., "A Future with Hybrid Electric Propulsion Systems: A NASA Perspective," in Turbine Engine Technology Symposium (No. GRC-E-DAA-TN17600), September 2014.

[10] Fornaro, E., Cardone, M., and Dannier, A., "A Comparative Assessment of Hybrid Parallel, Series, and Full-Electric Propulsion Systems for Aircraft Application," IEEE Access 10 (2022): 28808-28820.

[11] Voskuijl, M., Van Bogaert, J., and Rao, A.G., "Analysis and Design of Hybrid Electric Regional Turboprop Aircraft," CEAS Aeronautical Journal 9 (2018): 15-25.

[12] CMD s.p.a. a Loncin Company Via Pacinotti 2. San Nicola la Strada CE. Italy. https://www.cmdengine.com/divisioni/avio/

[13] EMRAX d.o.o. Molkova pot 5 SI-1241 Kamnik Slovenia. EU https://www.cmdengine.com/divisioni/avio/

[14] Vukosavic. S. N. (2012). Electrical machines. Springer Science & Business Media.

[15] ITECH Electronic Co.. Ltd. China. https://www.itechate.com/en/download.html

[16] Cardone, M., Gargiulo, B., & Fornaro, E. (2021, July). Development of a flexible test bench for a Hybrid Electric Propulsion System. In 2021 IEEE International Workshop on Metrology for Automotive (MetroAutomotive) (pp. 221-225). IEEE.

[17] Fornaro, E., Cardone, M., & Dannier, A. (2022, June). Hybrid Electric Aircraft Model Based on ECMS Control. In 2022 International Symposium on Power Electronics, Electrical Drives, Automation and Motion (SPEEDAM) (pp. 865-870). IEEE.

[18] Cardone. M.. Gargiulo. B.. & Fornaro. E. (2021). Modelling and experimental validation of a hybrid electric propulsion system for light aircraft and unmanned aerial vehicles. Energies. 14(13). 3969.

[19] Mathworks: MATLAB. Mapped SI Engine. Natick. Massachusetts: The MathWorks Inc. (2023). https://it.mathworks.com/help/autoblks/ref/mappedsiengine.html

[20] Mathworks: MATLAB. Mapped Motor. Natick. Massachusetts: The MathWorks Inc. (2023). https://it.mathworks.com/help/autoblks/ref/mappedmotor.html

[21] Mathworks: MATLAB. Generic Battery Model. Natick. Massachusetts: The MathWorks Inc. (2023). https://it.mathworks.com/help/sps/powersys/ref/battery.html

[22] Iodice. P.. Fornaro. E.. & Cardone. M. (2022). Hybrid Propulsion in SI Engines for New Generation Motorcycles: A Numerical-Experimental Approach to Assess Power Requirements and Emission Performance. Energies. 15(17). 6312.

[23] Iodice, P., Fornaro, E., & Cardone, M. (2022, December). Hybrid propulsion for motorcycle application to reduce engine-out emissions: an analytical-experimental investigation. In Journal of Physics: Conference Series (Vol. 2385, No. 1, p. 012065). IOP Publishing.

[24] Energy, S. (2012). Panasonic NCR18650B.